

# Multiplicity dependent $p_T$ distributions of identified particles in pp collisions at 7 TeV within HIJING/ $B\bar{B}$ v2.0 model

V. Topor Pop<sup>1,2</sup> and M. Petrovici<sup>2,\*</sup>

<sup>1</sup>*Physics Department, McGill University, Montreal, Canada, H3A 2T8*

<sup>2</sup>*National Institute for Physics and Nuclear Engineering-Horia Hulubei*

*Hadron Physics Department*

*R-077125, Bucharest, Romania*

(Dated: June 24, 2019)

Effects of strong longitudinal color fields (SCF) on the identified (anti)particle transverse momentum ( $p_T$ ) distributions in  $pp$  collision at  $\sqrt{s} = 7$  TeV are investigated within the framework of the HIJING/ $B\bar{B}$  v2.0 model. The comparison with the experiment is performed in terms of the correlation between mean transverse momentum ( $\langle p_T \rangle$ ) and multiplicity ( $N_{ch}^*$ ) of charged particles at central rapidity, as well as the ratios of the  $p_T$  distributions to the one corresponding to the minimum bias (MB)  $pp$  collisions at the same energy, each of them normalized to the corresponding charged particle density, for high multiplicity (HM,  $N_{ch} > 100$ ) and low multiplicity (LM,  $N_{ch} < 100$ ) class of events. The theoretical calculations show that an increase of the strength of color fields (as characterized by the effective values of the string tension  $\kappa$ ), from  $\kappa = 2$  GeV/fm to  $\kappa = 5$  GeV/fm from LM to HM class of events, respectively, lead to a ratio at low and intermediate  $p_T$  (*i.e.*,  $1\text{GeV}/c < p_T < 6\text{GeV}/c$ ) consistent with recent data obtained at LHC by the ALICE Collaboration. These results point out to the necessity of introducing a multiplicity (or energy density) dependence for the effective value of the string tension. Moreover, the string tension  $\kappa = 5$  GeV/fm, describing the  $p_T$  spectra of ID (anti)particle in  $pp$  collisions at  $\sqrt{s} = 7$  TeV for high charged particle (HM) multiplicity event classes, has the same value as the one used in describing the  $p_T$  spectra in central Pb - Pb collisions at  $\sqrt{s_{NN}} = 2.76$  TeV. Therefore, we can conclude that at the LHC energies the global features of the interactions could be mostly determined by the properties of the initial chromoelectric flux tubes, while the system size may play a minor role.

PACS numbers: 25.75.Dw, -25.75.-q, 25.75.Gz, 13.85.-t

## I. INTRODUCTION

Relativistic and ultra-relativistic heavy-ion experimental data evidenced global features such as flow, baryon-meson anomaly, (multi)strange enhancement, jet quenching which support the interpretation within theoretical (phenomenological) models as originating from a deconfined, strongly interacting thermalised phased, coined Quark-Gluon Plasma (sQGP). A recent review was presented at the Quark Matter Conference 2017 [1, 2]. In contrast, no similar effects were observed in proton-proton ( $pp$ ) and proton-nucleus ( $p - A$ ) collisions, these results being considered of interest only as reference data for nucleus-nucleus ( $A - A$ ) collisions. Recently, features reminiscent from heavy-ion phenomenology have been found also in such reactions at the LHC energies, *i.e.*, long range near side ridge in particle correlations observed in high multiplicity events [3–6], collective flow [7–9], or strangeness enhancement [10]. The nature of these similarities is still an open question. Do they originate from a deconfined phase following a hydrodynamic evolution like in nucleus-nucleus ( $A - A$ ) collisions or are they a consequence of the initial state dynamics manifested in the final state observables [7, 11–13]? Most

probable the two processes coexist, with a dense thermalised central core and an outer corona. Such a picture is successfully implemented in the EPOS model (Energy sharing Parton based theory with Off-shell remnants and ladder Splitting)[14–16]. The core-corona interplay in the light flavor hadron production for Pb - Pb collisions at  $\sqrt{s_{NN}} = 2.76$  TeV was recently discussed in Ref. [17]. Therefore, the study of  $pp$ ,  $p - A$  and  $A - A$  collisions as function of charged particle multiplicity has gathered recently much attention [1, 12, 13, 18–23].

The non-perturbative particle creation mechanisms in strong external fields has a wide range of application not only in the original  $e^+e^-$  pair creation on quantum electrodynamics (QED) problems [24], but also for pair creation (fermions and bosons) in strong non-Abelian electromagnetic fields [25–36]. In a high-energy heavy-ion collision, strong color fields are expected to be produced between the partons of the projectile and target. Theoretical descriptions of particle production in high energy  $pp$  and  $A - A$  collisions are based on the introduction of chromoelectric flux tube (*strings*) models [37–39]. String breaking picture [37] is a good example of how to convert the kinetic energy of a collisions into field energy. Therefore, Schwinger mechanism [24] for non-perturbative particle production in strong color fields is assumed to play an important role in the dynamics of the  $pp$  and nucleus-nucleus ( $A - A$ ) collisions.

In a string fragmentation phenomenology, it has

\* mpetro@nipne.ro

been proposed that the observed strong enhancement of strange particle production in nuclear collisions could be naturally explained via strong longitudinal color field effects (SLCF) [26]. Recently, an extension of color Glass Condensate (CGC) theory has proposed a more detailed dynamical model of color ropes “GLASMA” [40–42].

In the string models, strong longitudinal fields (flux tubes, effective strings) decay into new ones by quark anti-quark ( $q\bar{q}$ ) or diquark anti-diquark ( $qq\text{--}\bar{q}\bar{q}$ ) pair production and subsequently hadronize to produce the observed hadrons. Due to confinement, the color of these strings is restricted to a small area in transverse space [30]. With increasing energy of the colliding particles, the number of strings grows and they start to overlap, forming clusters. This can introduce a possible dependence of particle production on the energy density [43]. The effect of modifying the string tension due to local density has been studied in Monte Carlo models, which are used primarily for heavy-ion collisions [44–49]. In the Partons String Models (PSM) string fusion and percolation effects on strangeness and heavy flavor production have also been discussed in Refs. [50–53]. A similar model with string fusion into color ropes is considered in the Dipole evolution in Impact Parameter Space and rapidity (DIPSY) ([13, 54, 55]. String collective effects were also introduced in a multi-pomeron exchange model to improve the production of hadrons in  $pp$  collisions at the LHC energies [56–58].

Heavy Ion Jet Interacting (HIJING) type models such as HIJING1.0 [38, 39], HIJING2.0 [59, 60] and HIJING/B $\bar{B}$  v2.0 [61–71], have been developed to study hadron productions in  $pp$ ,  $p - A$  and  $A - A$  collisions. These models are based on a two-component geometrical model of mini-jet production and soft interaction and has incorporated nuclear effects such as *shadowing* (nuclear modification of the parton distribution functions) and *jet quenching*, via final state jet medium interaction. In the HIJING/B $\bar{B}$  v2.0 model [63, 65] we introduced new dynamical effects associated with long range coherent fields (*i.e.*, strong longitudinal color fields, SCF), including baryon junctions and loops [62, 72]. At RHIC energies we have shown [61–63] that the dynamics of strangeness production deviates considerably from calculations based on Schwinger-like estimates for homogeneous and constant color fields [24], and points to a possible contribution of fluctuations of transient strong color fields (SCF). These fields are similar to those which could appear in a *GLASMA* [41] at initial stage of the collisions. In a scenario with QGP phase transitions the typical field strength of SCF at ultra-relativistic energies was estimated to be about 5–12 GeV/fm [73].

The HIJING/B $\bar{B}$  v2.0 model has successfully described the global observables and identified particle (ID) data, including (multi)strange particles production in  $pp$  [65, 66, 69]  $p - Pb$  [68, 70, 71] and  $Pb - Pb$  collisions [67] at the LHC energies. However, correlations among different measurable quantities in multi-particle production offer a better way to constrain the models. In this paper we

extend our study to identified particle (*i.e.*,  $\pi$ ,  $K$ ,  $p$ ,  $\Lambda$ ,  $\Xi$ ,  $\Omega$  and their anti-particle) produced in the collisions of the small system. We will perform a detailed analysis of correlations between average transverse momentum  $\langle p_T \rangle$  and charged particles multiplicity ( $N_{ch}^*$ ) and for the ratio of double differential cross sections normalized to the charged particle densities ( $dN_{ch}/d\eta$ ) versus multiplicity, *i.e.*,

$$R_{mb} (cen) = \left( \frac{\frac{d^2 N}{dy dp_T}}{\langle \frac{dN_{ch}}{d\eta} \rangle} \right)_i^{cen} / \left( \frac{\frac{d^2 N}{dy dp_T}}{\langle \frac{dN_{ch}}{d\eta} \rangle} \right)_i^{ppMB} \quad (1)$$

where  $i$  = identified particle in  $pp$  collisions, “cen” stand for multiplicity event classes. We will consider high multiplicity (HM;  $N_{ch} > 100$ ), and low multiplicity (LM;  $N_{ch} < 100$ ) classes. MB stand for minimum bias events. The charged particle densities  $dN_{ch}/d\eta$  are integrated values at mid-pseudo-rapidity  $|\eta| < 0.5$  for that class of events. The  $p_T$  distributions of ID particle were recently measured in  $pp$  collisions at  $\sqrt{s} = 7$  TeV for different multiplicity classes of events by ALICE Collaboration [74–76].

## II. OUTLINE OF HIJING/B $\bar{B}$ V2.0 MODEL.

### A. Strong color field. String tension.

In this paper we present the results of calculations for different observables measured in  $pp$ ,  $p - Pb$  and  $Pb - Pb$  collisions at the LHC energies. Therefore, we consider useful for the reader to include a summary of the main input parameters which have been determined in Refs. [66] and that are used in the present analysis.

For a uniform chromoelectric flux tube with field ( $E$ ), the production rate for a quark pair ( $q\bar{q}$ ), per unit volume is given by [26, 77, 78]

$$\Gamma = \frac{\kappa^2}{4\pi^3} \exp \left( -\frac{\pi m_q^2}{\kappa} \right), \quad (2)$$

A measurable rate for spontaneous pair production requires strong chromoelectric fields, such that  $\kappa/m_q^2 > 1$ . Introducing strong longitudinal electric field within string models, results in a highly suppressed production rate of heavy  $Q\bar{Q}$  pair ( $\gamma_{Q\bar{Q}}$ ) related to light quark pairs ( $q\bar{q}$ ). From Eq. 2 one obtains the suppression factor  $\gamma_{Q\bar{Q}}$  [77]:

$$\gamma_{Q\bar{Q}} = \frac{\Gamma_{Q\bar{Q}}}{\Gamma_{q\bar{q}}} = \exp \left( -\frac{\pi(m_Q^2 - m_q^2)}{\kappa} \right), \quad (3)$$

The suppression factors are calculated for  $Q = qq$  (diquark),  $Q = s$  (strange),  $Q = c$  (charm), or  $Q = b$  (bottom) ( $q = u, d$  stand for light quarks).

The current quark masses are:  $m_s = 0.12$  GeV,  $m_c = 1.27$  GeV,  $m_b = 4.16$  GeV [79], and for di-quark  $m_{qq} = 0.45$  GeV [80]. The constituent quark masses of light non-strange quarks are  $M_{u,d} = 0.23$  GeV, of the strange quark is  $M_s = 0.35$  GeV [81], and of the diquark is  $M_{qq} = 0.55 \pm 0.05$  GeV [80]. In our calculations, we use  $M_{qq}^{\text{eff}} = 0.5$  GeV,  $M_s^{\text{eff}} = 0.28$  GeV,  $M_c^{\text{eff}} = 1.27$  GeV. Therefore, for the vacuum string tension value  $\kappa_0 = 1$  GeV/fm, the above formula from Eq. 3 results in a suppression of heavier quark production pair according to  $u\bar{u} : d\bar{d} : q\bar{q} : s\bar{s} : c\bar{c} \approx 1 : 1 : 0.02 : 0.3 : 10^{-11}$  [69]. For a color rope, on the other hand, if the effective string tension value  $\kappa$  increases to  $\kappa = f_\kappa \kappa_0$  (with  $f_\kappa > 1$ ) the value of  $\gamma_{Q\bar{Q}}$  increases. Equivalently, a similar increase of  $\gamma_{Q\bar{Q}}$  could be obtained by a decrease of quark mass from  $m_Q$  to  $m_Q/\sqrt{f_\kappa}$ . We have shown that this dynamical mechanism improves considerably the description of the strange meson/hyperon data at the Tevatron and at LHC energies [65]. The flux tubes used to simulate  $A-A$  collisions may have a string tension almost one order of magnitude larger than the fundamental string tension linking a mesonic quark-antiquark pair [25, 30].

The initial energy densities in the collisions ( $\epsilon_{\text{ini}}$ ) are computed from the square of the field components [30]. Within our phenomenology  $\epsilon_{\text{ini}}$  is proportional to mean field values  $\langle E^2 \rangle$ , and using the relation  $\kappa = e_{\text{eff}} E$ , results  $\epsilon_{\text{ini}} \propto \kappa^2$ . Using Bjorken relation the  $\epsilon_{\text{ini}}$  is proportional with charged particle density at mid-rapidity and therefore  $\kappa^2 \propto (dN_{\text{ch}}/d\eta)_{\eta=0}$ . A similarity with the phenomenology embedded in the CGC model is obvious, and we obtain  $\kappa \propto Q_{\text{sat},p}$  as discussed in Ref. [66]. In Ref. [66], in order to describe the energy dependence of the charged particle density at mid rapidity in  $pp$  collisions up to the LHC energies, we used a power law dependence:

$$\kappa(s) = \kappa_0 (s/s_0)^{0.04} \text{ GeV/fm}, \quad (4)$$

consistent (within the error) with the value deduced also in CGC model for  $Q_{\text{sat},p}$  [82].

Equation 4 leads to an increasing value for the effective string tension value from  $\kappa = 1.5$  GeV/fm at  $\sqrt{s} = 0.2$  TeV (top RHIC energy) to  $\kappa = 2.0$  GeV/fm at  $\sqrt{s} = 7$  TeV. The sensitivity to the string tension values ( $\kappa$ ) for different observables have been studied in previous papers [62–65, 67, 69].

Our phenomenological parametrizations Eq. 4, is strongly supported by data on charged particle densities at mid-rapidity  $(dN_{\text{ch}}/d\eta)_{\eta=0}$ . Within the error the  $\sqrt{(dN_{\text{ch}}/d\eta)_{\eta=0}}$  shows a power law dependence proportional to  $s^{0.05}$  for inelastic  $pp$  interactions and to  $s^{0.055}$  for non-single diffractive events [83, 84].

In addition, in  $A-A$  collisions the effective string tension value could also increase due to in-medium effects [67], or dependence on the number of participants. This increase is quantified in our phenomenology by an analogy with CGC model. We consider for the mean value of the string tension an energy and mass dependence,  $\kappa(s, A) \propto Q_{\text{sat},A}(s, A) \propto Q_{\text{sat},p}(s)A^{1/6}$ . There-

fore, we use in the present analysis for  $A-A$  collisions a power law dependence  $\kappa = \kappa(s, A)$

$$\kappa(s, A)_{\text{LHC}} = \kappa(s)A^{0.167} = \kappa_0 (s/s_0)^{0.04}A^{0.167} \text{ GeV/fm}, \quad (5)$$

Eq. 5 leads to  $\kappa(s, A)_{\text{LHC}} \approx 5$  GeV/fm, in Pb - Pb collisions at c.m. energy per nucleon  $\sqrt{s_{NN}} = 2.76$  TeV. Note that the suppression factors  $\gamma_{Q\bar{Q}}$ , approach unity in Pb - Pb collisions at  $\sqrt{s_{NN}} = 2.76$  TeV, for the string tension values  $\kappa \geq 5$  GeV/fm.

The mean effective values of the string tension  $\kappa(s)$  for  $pp$  collisions (Eq. 4) and  $\kappa(s, A)$  for Pb - Pb collisions (Eq. 5) are used in the present calculations. These lead to an increase of the various suppression factors, as well as an enhancement of the intrinsic (primordial) transverse momentum  $k_T$ , *i.e.* : i) the ratio of production rates of diquark-quark to quark pairs (diquark-quark suppression factor),  $\gamma_{qq} = \Gamma(qq\bar{q}\bar{q})/\Gamma(q\bar{q})$ ; ii) the ratio of production rates of strange to non-strange quark pairs (strangeness suppression factor),  $\gamma_s = \Gamma(s\bar{s})/\Gamma(q\bar{q})$ ; iii) the extra suppression associated with a diquark containing a strange quark compared to the normal suppression of strange quark ( $\gamma_s$ ),  $\gamma_{us} = (\Gamma(us\bar{u}\bar{s})/\Gamma(ud\bar{u}\bar{d})) / (\gamma_s)$ ; iv) the suppression of spin 1 di-quarks relative to spin 0 ones (in addition to the factor of 3 enhancement of the former based on counting the number of spin states),  $\gamma_{10}$ ; and v) the (anti)quark ( $\sigma_q'' = \sqrt{\kappa/\kappa_0} \cdot \sigma_q$ ) and (anti)diquark ( $\sigma_{qq}'' = \sqrt{\kappa/\kappa_0} \cdot f \cdot \sigma_{qq}$ ) Gaussian width of primordial (intrinsic) transverse momentum  $k_T$ . In the above formula for  $\sigma_q''$  and  $\sigma_{qq}''$  we use  $\sigma_q = \sigma_{qq} = 0.350$  GeV/c as default values (in absence of SCF effects) for Gaussian width of quark (diquark) intrinsic transverse momentum distribution. Note, that the factor  $f = 3$ , has been discussed in Ref. [65, 66].

Moreover, for a better description of the baryon/meson anomaly seen in data at RHIC and LHC energies, a specific implementation of  $J\bar{J}$  loops, had to be introduced (for details see Refs. [67, 69]). The absolute yield of charged particles,  $dN_{\text{ch}}/d\eta$  is also sensitive to the low  $p_T < 2$  GeV/c non-perturbative hadronization dynamics that is performed via LUND [85] string JETSET [86] fragmentation as constrained from lower energy  $ee$ ,  $ep$ ,  $pp$  data. The conventional hard pQCD mechanisms are calculated in HIJING/B $\bar{B}$  v2.0 via the PYTHIA [87] subroutines. Nuclear shadowing and jet quenching are discussed in Ref. [66].

The main advantage of HIJING/B $\bar{B}$  v2.0 over PYTHIA 6.4 is the ability to include novel SCF color rope effects that arise from longitudinal fields amplified by the random walk in color space of the high  $x$  valence partons in  $A-A$  collisions. This random walk could induce a very broad fluctuation spectrum of the effective string tension. In the present work we will study only the effect of a larger effective value  $\kappa > 1$  GeV/fm on the production of identified particles measured in Pb - Pb,  $p$  - Pb and  $pp$  collisions at LHC energies. The model is based on the time-independent strength of color field while in reality the production of  $Q\bar{Q}$  pairs is a far-from-equilibrium,

time and space dependent complex phenomenon. Therefore, we can not investigate in details possible fluctuations which could appear due to these more complex dependencies.

### III. NUMERICAL RESULTS AND DISCUSSION

#### A. The average transverse momentum $\langle p_T \rangle$ versus $N_{ch}$ correlations

The HIJING/B $\bar{B}$  v2.0 model predicts many experimental observables (charged hadron pseudo-rapidity distributions, transverse momentum spectra, identified particle spectra, baryon-to-meson ratios) using the above values for the effective string tension,  $\kappa$  (see Sec. II) [65, 66, 68–70].

The ALICE Collaboration has reported measurements of the average transverse momentum  $\langle p_T \rangle$  versus charged particles  $N_{ch}^*$  at central rapidity in  $pp$  at  $\sqrt{s} = 7$  TeV,  $p$ -Pb at  $\sqrt{s_{NN}} = 5.02$  TeV, and Pb - Pb collisions at  $\sqrt{s_{NN}} = 2.76$  TeV [88]. The analysis range was restricted to a transverse momentum  $0.15 < p_T < 10$  GeV/ $c$  and to a mid-pseudo-rapidity range  $|\eta| < 0.3$ . Figure 1 shows the results obtained with HIJING/B $\bar{B}$  v2.0 model (open symbols) for  $pp$  collisions at  $\sqrt{s} = 7$  TeV (left panel) and  $p$ -Pb at  $\sqrt{s_{NN}} = 5.02$  TeV (right panel). As we can see in Fig. 1 a continuous increase of  $\langle p_T \rangle$  with  $N_{ch}^*$  is observed for both reactions. Therefore, to calculate the correlation  $\langle p_T \rangle_{N_{ch}}$  vs  $N_{ch}^*$ , we first investigate in a model of hadronizing strings if the above increase could be attributed to the effects of SCF and the results are given for different strength of color fields quantified by an effective value of the string tension from  $\kappa = 1$  GeV/fm (default value) up to  $\kappa = 5$  GeV/fm. As we could remark, the calculations with the default value  $\kappa = 1$  GeV/fm, describe better the  $pp$  data. An alternative explanation of the increase of  $\langle p_T \rangle$  with  $N_{ch}^*$  should be naturally given in the context of the fragmentation of multiple minijets embedded in HIJING type models [38] and was discussed in the early 90s for  $p\bar{p}$  collisions at  $\sqrt{s} = 1.8$  TeV [39]. The large multiplicity events are dominated by multiple minijets while low multiplicity events are dominated by those of no jet production. Few partons are enough to explain the increase of  $\langle p_T \rangle$  with  $N_{ch}^*$ . We may also conclude that these correlations in  $pp$  collisions at  $\sqrt{s} = 7$  TeV are not sensitive to the soft fragmentation region, where we expect that SCF effects are dominant. In contrast, for  $p$ -Pb collisions the theoretical calculations compared to data [88] in Fig. 1 (right panel) show better agreement if the value of  $\kappa$  is increased from  $\kappa = 1$  GeV/fm to  $\kappa = 3$  GeV/fm.

We will study now the effect of an enhanced value of the effective string tension  $\kappa$  on the correlation of  $\langle p_T \rangle$  versus  $N_{ch}^*$  for ID particle in  $pp$  and  $p$ -Pb collisions at  $\sqrt{s} = 7$  TeV, and  $\sqrt{s_{NN}} = 5.02$  TeV, respectively. Shown in Fig. 2 are our theoretical calculations (open symbols) in comparison with data [74, 75] on the  $\langle p_T \rangle$  of  $\pi^+ + \pi^-$ ,

$K^+ + K^-$ ,  $p + \bar{p}$ ,  $\Xi^- + \bar{\Xi}^+$ , and  $\Omega^- + \bar{\Omega}^+$  for  $0 < p_T < 10$  GeV/ $c$  and mid-rapidity  $|y| < 0.5$  versus charged particle multiplicity  $N_{ch}^*$  (selected in the  $|\eta| < 0.5$  range) for  $pp$  collisions at  $\sqrt{s}=7$  TeV. The results (open symbols) are given for two values of the effective string tension  $\kappa = 2$  GeV/fm (left panel) and  $\kappa = 5$  GeV/fm (right panel). The data show an increase of  $\langle p_T \rangle$  with increased multiplicity and with the particle mass, facts fairly well described by the model. Note, that for clarity we did not include here the results for  $\Lambda + \bar{\Lambda}$ . Since the mass difference between lambda and proton is very small, the results are almost the same [74]. The  $\langle p_T \rangle$  increases with increasing multiplicity as the effect of the strong color field (SCF) embedded in our model. A modified string fragmentation using  $\kappa = 2$  GeV/fm increase the production rate for heavier particle production. Moreover an increase of the width of the primordial (intrinsic) transverse momentum ( $k_T$ ) distribution from the default value of the Gaussian ( $\sigma_q = \sigma_{qq} = 0.350$  GeV/ $c$ ) to larger values for the (anti)quark ( $\sigma_q'' = \sqrt{\kappa/\kappa_0} \cdot \sigma_q$ ) and (anti)diquark ( $\sigma_{qq}'' = \sqrt{\kappa/\kappa_0} \cdot f \cdot \sigma_{qq}$ ), where  $f = 3$  [65, 66], contribute also to an increases of the heavier particle production rate. This provides a consistent evidence that modified fragmentation obtained by an enhanced  $\kappa$  from the default value  $\kappa = 1$  GeV/fm and minijet production as implemented in HIJING/B $\bar{B}$  v2.0 model lead to a fairly good description of these observables. However, the model give only partial agreement of  $\langle p_T \rangle$  values for ID particle at high multiplicity. The model describes well  $\langle p_T \rangle$  of  $\pi^+ + \pi^-$ ,  $p + \bar{p}$ ,  $\Lambda + \bar{\Lambda}$ , but the results strongly underestimate the  $\langle p_T \rangle$  of (multi)strange particles as  $K^+ + K^-$ , and  $\Xi^- + \bar{\Xi}^+$ , and  $\Omega^- + \bar{\Omega}^+$ . We studied if one can find a scenario that would give a larger enhancement of the  $\langle p_T \rangle$  of (multi)strange particles. We consider the effect of a further increase of the string tension to  $\kappa = 5$  GeV/fm and the results are presented in Fig. 2 (right panel).

Note that a value  $\kappa \approx 5\kappa_0$  GeV/fm is also supported by the calculations at finite temperature ( $T$ ) of potentials associated with a  $q\bar{q}$  pair separated by a distance  $r$  [89]. The finite temperature ( $T$ ) form of the  $q\bar{q}$  potential has been calculated by means of lattice QCD [90]. At finite temperature, there are two potentials associated with a  $q\bar{q}$  pair separated by a distance  $r$ : the free energy  $F(T, r)$  and internal energy  $V(T, r)$ . The free and internal energies actually correspond to slow and fast (relative) motion of the charges, respectively. Infrared sensitive variables such as string tension are very helpful to identify specific degrees of freedom of the plasma. Since the confinement of color in non-Abelian theories is due to the magnetic degree of freedom, the magnetic component is expected to be present in the plasma as well. In the presence of the *chromo-magnetic scenario* it was shown that the effective string tension of the free energy  $\kappa = \kappa_F$  decreases with  $T$ , to near zero at critical temperature ( $T_c$ ). In contrast, the effective string tension of the internal energy (corresponding to a fast relative motion of the charges)  $\kappa = \kappa_V$  remains nonzero below  $\sim T = 1.3 T_c$  with a peak value at  $T_c$  about 5 times the vacuum tension

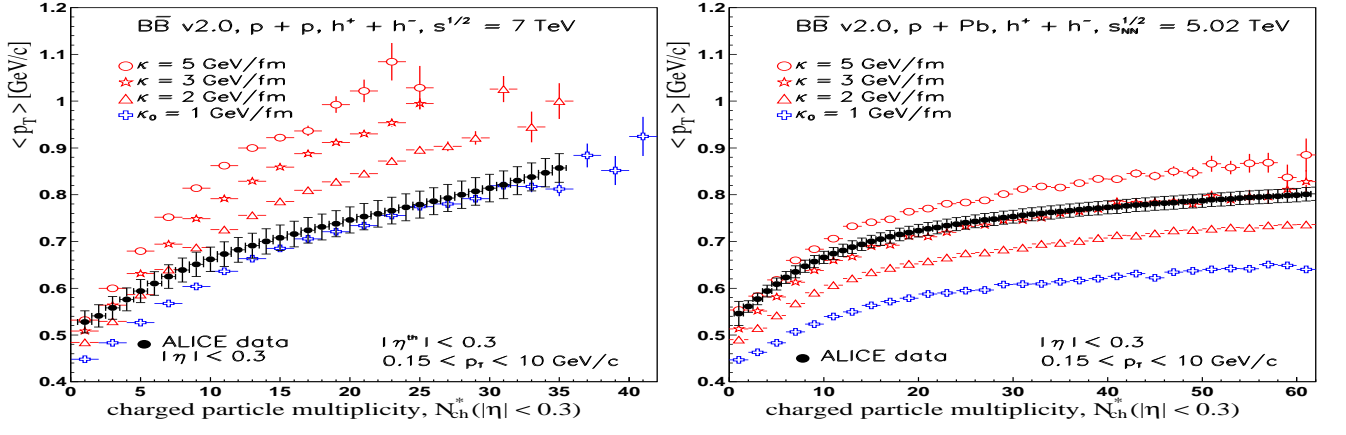


FIG. 1. Open symbols-HIJING/B $\bar{b}$  v2.0 predictions for the average transverse momentum ( $\langle p_T \rangle$ ) of charged particles as a function of multiplicity at mid-pseudo-rapidity  $N_{ch}^*$ . Left panel- $pp$  collisions at  $\sqrt{s} = 7$  TeV for  $0.15 < p_T < 10$  GeV/c and mid-pseudo-rapidity  $|\eta| < 0.3$ ; Right panel- $p$  - Pb collisions at  $\sqrt{s_{NN}} = 5.02$  TeV for  $0.15 < p_T < 10$  GeV/c and mid-rapidity  $|\eta| < 0.3$ . The theoretical results are obtained for different effective string tensions increasing from  $\kappa = 1$  GeV/fm (default) up to  $\kappa = 5$  GeV/fm. The ALICE data (filled circles) are from Ref. [88]. The errors represent systematic uncertainties on  $\langle p_T \rangle$ . The statistical errors are negligible.

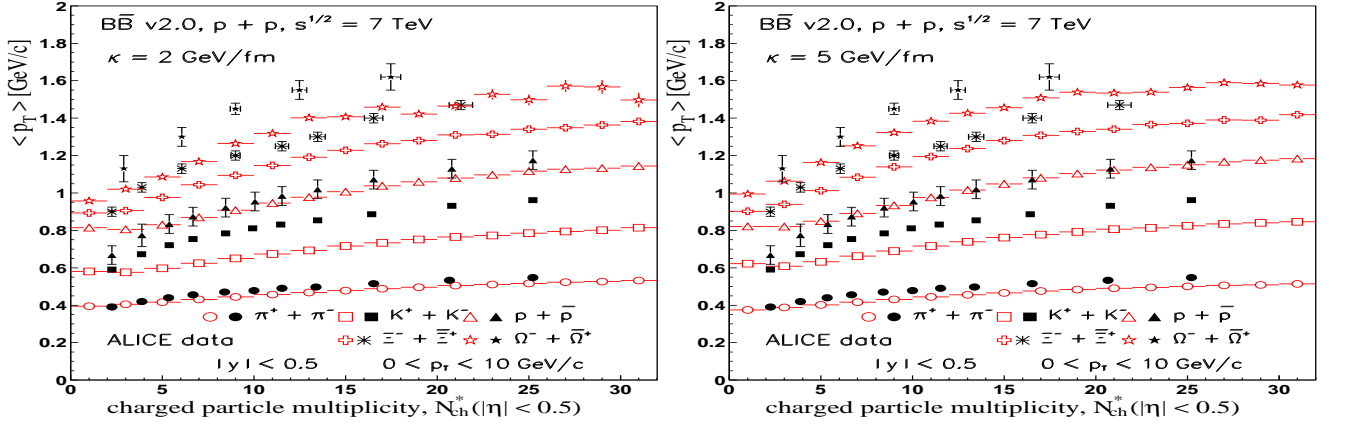


FIG. 2. Open symbols-HIJING/B $\bar{b}$  v2.0 predictions for the average transverse momentum ( $\langle p_T \rangle$ ) of identified particle for  $0 < p_T < 10$  GeV/c and mid-rapidity  $|\eta| < 0.5$  as function of charged particle multiplicity,  $N_{ch}^*$  in  $pp$  collisions at  $\sqrt{s} = 7$  TeV. The results are obtained with an effective string tension value,  $\kappa = 2$  GeV/fm (left side) and  $\kappa = 5$  GeV/fm (right side). For clarity we do not include the results for  $\Lambda$ . The ALICE preliminary data (filled symbols) are from Ref. [74, 75]. Only statistical error bars are shown.

$\kappa_0$  ( $\kappa_V = 5$   $\kappa_0 = 5$  GeV/fm) [89].

The above calculations for  $\kappa \approx 5\kappa_0$  GeV/fm result in only a modest increase of the  $\langle p_T \rangle$  of kaons ( $K^+ + K^-$ ) by 10-15 % and a better description of  $\langle p_T \rangle$  of multi-strange particles ( $\Xi^- + \bar{\Xi}^-$  and  $\Omega^- + \bar{\Omega}^-$ ) only at low multiplicity ( $N_{ch} < 15$ ). In our calculations the discrepancy obtained for  $\langle p_T \rangle$  of kaons does not appear to turn over for  $\kappa = 5$  GeV/fm as expected. This discrepancy may be related to the kaon enhancement reported first in Ref. [93] at Tevatron energies and confirmed now at LHC energies [74, 75]. Note, that new PYTHIA8 model which include a specific increase of the string tension values [12], also could not describe better the  $\langle p_T \rangle$  of kaons in  $pp$  collisions

at  $\sqrt{s} = 7$  TeV. Further analysis are necessary in order to draw a definite conclusion.

In the HIJING/B $\bar{b}$  v2.0 model the collective behavior is a consequence of the confining strong color fields, resulting in an interaction between strings that is without diffusion or loss of energy [13]. Therefore, for values of string tension between 5 and 10 GeV/fm (the calculations are not included here) a saturation seems to set in, possibly as an effect of energy and momentum conservation, as well as due to a saturation of strangeness suppression factors. Similar conclusions could be drawn for  $\langle p_T \rangle$  of ID particles versus charged particle multiplicity,  $N_{ch}^*$  measured in  $p$  - Pb collisions at  $\sqrt{s_{NN}} = 5.02$  TeV.

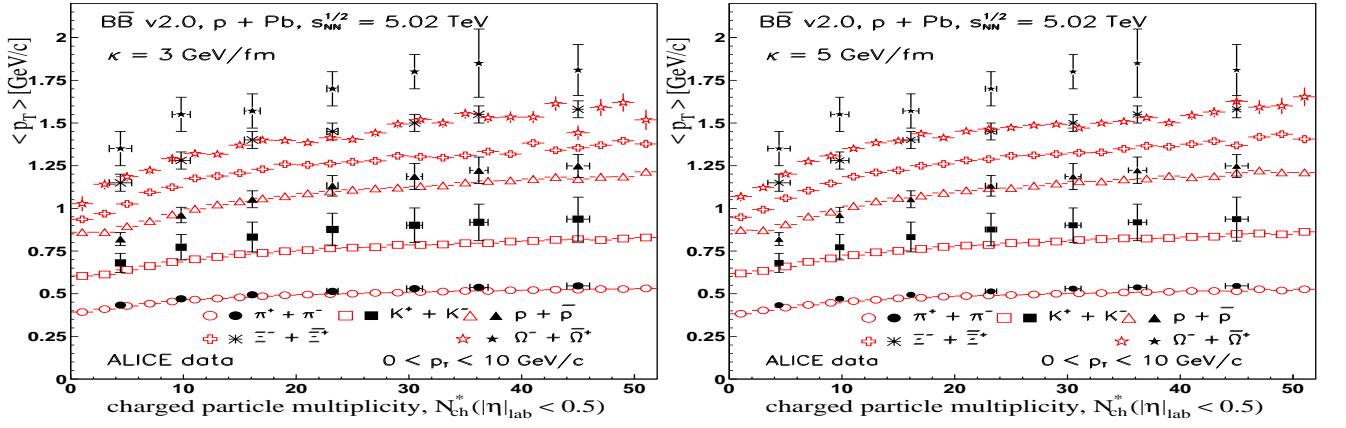


FIG. 3. Open symbols - HIJING/BB v2.0 predictions for the average transverse momentum ( $\langle p_T \rangle$ ) of identified particle in the range  $0 < p_T < 10$  GeV/c and mid-rapidity  $0.0 < y_{cm} < 0.5$  as function of charged particle multiplicity,  $N_{ch}^*$  in p - Pb collisions at  $\sqrt{s_{NN}} = 5.02$  TeV. The results (open symbols) are obtained with an effective string tension value,  $\kappa = 3$  GeV/fm (left side), and  $\kappa = 5$  GeV/fm (right side). For clarity we do not include the results for  $\Lambda$ . The ALICE data (filled symbols) are from Ref. [91]. Only statistical error bars are shown.

The results (open symbols) are obtained in the range  $0 < p_T < 10$  GeV/c and mid-rapidity  $0.0 < y_{cm} < 0.5$ , and are shown in Fig. 3.

Up to now, the microscopic origin of enhanced (multi)strange particles production is not known. It is, therefore, a valid question whether small systems (high multiplicity  $pp$  and  $p$  - Pb) exhibit any behavior of the kind observed in heavy-ion collisions. Bjorken suggested the possibility of deconfinement in  $pp$  collisions [94]. Van Hove [95] and Campanini [96] suggested that an anomalous behavior of average transverse momentum ( $\langle p_T \rangle$ ) as a function of multiplicity could be a signal for the occurrence of a phase transition in hadronic matter, *i.e.*, formation of a *mini quark-gluon plasma* (mQGP). The long range near side ridge in particle correlations observed in high multiplicity events [3–6], collective flow [7–9] and strangeness enhancement [10] were evidenced in  $pp$  collisions at the LHC energies and support such hypothesis.

However, a fundamental question remains, are such correlation of  $\langle p_T \rangle$  vs  $N_{ch}^*$  for ID particle in small systems ( $pp$ ,  $p$  - Pb collisions) of collective origin, attributed to a hydrodynamic evolution like in Pb - Pb collisions, or they are a natural consequence due to initial state dynamics that show-up in the final state observables [13]?

Collective hydrodynamic flow as a signature of sQGP is well established in Pb - Pb collisions at LHC energies. Such conclusions can be drawn from measurements of the invariant yields of identified particles in central Pb - Pb collisions at  $\sqrt{s_{NN}} = 2.76$  TeV. In Fig. 4 we consider the results for light identified charged hadrons in Pb - Pb collisions (solid histograms) in comparison with those produced in  $pp$  collisions (dashed histograms) at  $\sqrt{s} = 2.76$  TeV. The experimental data are from ALICE Collaboration Ref. [98]. The calculation are performed taking an effective value of the string tension  $\kappa$  an energy and mass dependence as in Eq. 5, *i.e.*,

$\kappa(s, A)_{LHC} = \kappa(s)A^{0.167} = \kappa_0 (s/s_0)^{0.04}A^{0.167}$  GeV/fm. This formula leads to  $\kappa(s, A)_{LHC} \approx 5$  GeV/fm, in Pb - Pb collisions at c.m. energy per nucleon  $\sqrt{s_{NN}} = 2.76$  TeV. In  $pp$  collisions we consider only variation with energy, *i.e.*,  $\kappa(s) = \kappa_0 (s/s_0)^{0.04}$  GeV/fm, which gives a value of  $\kappa \approx 1.9$  GeV/fm. The results obtained within our model show a partial agreement with data, since a large pressure in the initial state, leading to flow especially for (anti)protons, is not considered in string fragmentation models.

## B. Ratio of normalized transverse momentum distributions

The measured transverse momentum distributions for ID particles for different multiplicity bins have been recently reported by ALICE Collaboration in  $pp$  collisions at  $\sqrt{s} = 7$  TeV [74–76]. The transverse momentum spectra of the identified hadrons (ID) were measured for several event multiplicity classes from the highest (class I) to the lowest (class X) multiplicity classes, corresponding to approximately 3.5 and 0.4 times the average value in the integrated sample ( $\langle dN_{ch}/d\eta \rangle^{MB} \approx 6.0$ ), respectively. In experiment the multiplicity classes are defined based on the total charge deposited in the V0A and V0C detectors located at forward ( $2.8 < \eta < 5.1$  and backward ( $-3.7 < \eta < -1.7$ ) pseudorapidity regions, respectively. The event multiplicity estimator is taken to be the sum of V0A and V0C signals denoted as V0M. The average charged particle density ( $\langle dN_{ch}^{exp}/d\eta \rangle$ ), is estimated within each multiplicity class by the average of the tracks distribution in the region  $|\eta| < 0.5$  [75, 76].

Based on these spectra and minimum bias results we will study here the ratio of double differential cross sections normalized to the charged particle densities

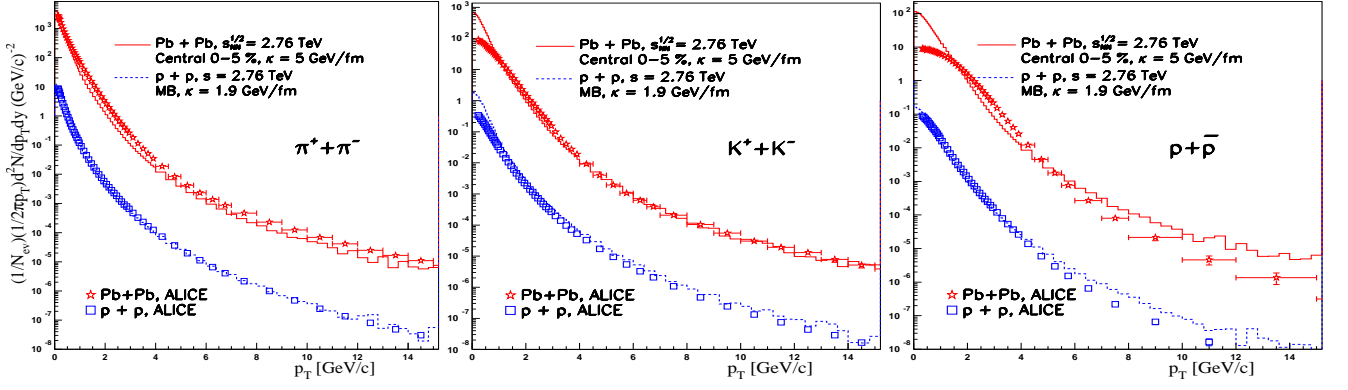


FIG. 4. (color online) HIJING/B $\bar{B}$  v2.0 predictions for the invariant yields of identified particles in central Pb -Pb collisions (solid histograms) and  $pp$  collisions (dashed histograms) at c.m. energy 2.76 TeV. The results are obtained using  $\kappa = 5$  GeV/fm ( $\kappa = 1.9$  GeV/fm) for Pb - Pb ( $pp$ ) respectively. The ALICE data are from Ref. [98]. The error include systematic uncertainties.

$dN_{ch}^{th}/d\eta$  versus multiplicity, *i.e.*, the ratio  $R_{mb}$  defined in Eq. 1.

For theoretical calculations within HIJING/B $\bar{B}$  v2.0 model we will chose different classes of event activity cutting on the total multiplicity ( $N_{ch}$ ) for each  $10^6$  set of events generated using two effective string tension values, *i.e.*,  $\kappa = 2.0$  GeV/fm and an enhanced value to  $\kappa = 5.0$  GeV/fm. Moreover, the average charged particle density, is estimated (for both set of events) within each multiplicity class of events, by the integrated value of  $dN_{ch}^{th}/d\eta$  at mid-pseudorapidity ( $|\eta| < 0.5$ ). In addition, we generate also  $10^6$  minimum bias (MB) events for  $\kappa = 2.0$  GeV/fm. Note, that for this selection theoretical calculations give an integrated charged particle density at mid-pseudorapidity ( $|\eta| < 0.5$ ),  $(dN_{ch}^{th}/d\eta)^{MB} = 5.7$ , close to the experimental value  $\langle dN_{ch}/d\eta \rangle^{MB} \approx 6.0$  quoted above.

We will consider six classes of event activity defined as:

- class I:  $200 \leq N_{ch} < 300$  ;  $dN_{ch}^{th}/d\eta = 30.9$  (for  $\kappa = 2$  GeV/fm);  $dN_{ch}^{th}/d\eta = 25.2$  (for  $\kappa = 5$  GeV/fm).
- class II:  $120 \leq N_{ch} < 200$  ;  $dN_{ch}^{th}/d\eta = 18.6$  (for  $\kappa = 2$  GeV/fm);  $dN_{ch}^{th}/d\eta = 15.1$  (for  $\kappa = 5$  GeV/fm).
- class III:  $100 \leq N_{ch} < 120$  ;  $dN_{ch}^{th}/d\eta = 12.5$  (for  $\kappa = 2$  GeV/fm);  $dN_{ch}^{th}/d\eta = 10.3$  (for  $\kappa = 5$  GeV/fm).
- class IV:  $80 \leq N_{ch} < 100$  ;  $dN_{ch}^{th}/d\eta = 9.7$  (for  $\kappa = 2$  GeV/fm);  $dN_{ch}^{th}/d\eta = 7.8$  (for  $\kappa = 5$  GeV/fm).
- class V:  $60 \leq N_{ch} < 80$  ;  $dN_{ch}^{th}/d\eta = 7.1$  (for  $\kappa = 2$  GeV/fm);  $dN_{ch}^{th}/d\eta = 5.7$  (for  $\kappa = 5$  GeV/fm).
- class VI:  $30 \leq N_{ch} < 60$  ;  $dN_{ch}^{th}/d\eta = 4.7$  (for  $\kappa = 2$  GeV/fm);  $dN_{ch}^{th}/d\eta = 3.9$  (for  $\kappa = 5$  GeV/fm).

For comparison to data from Refs. [75, 76] we show in Fig. 5, Fig. 6, and Fig. 7 the results of the HIJING/B $\bar{B}$

v2.0 predictions for transverse momentum distributions at mid-rapidity for light hadrons, *i.e.*,  $\pi, K, p$  and their anti-particles in two multiplicity classes, class I (panels a, b) and class V (panels c, d). The model estimates are represented by solid (dashed) histograms for  $\kappa = 2$  GeV/fm and  $\kappa = 5$  GeV/fm, respectively. For comparison with data, the experimental spectra (open stars) are chosen for an average value of  $\langle dN_{ch}^{exp}/d\eta \rangle$  similar with those obtained in the model,  $dN_{ch}^{th}/d\eta$  (see the above six classes of event activity). The results for minimum bias  $pp$  collisions obtained for  $\kappa = 2$  GeV/fm and represented by dotted histograms). Data for MB are from Ref. [92] (open circles) and Ref. [97] (open squares).

The ratio of double differential cross sections normalized to the charged particle densities,  $R_{mb}$  (calculated by us) is plotted for high (class I) and low (class V) multiplicity classes in panels e, f by dashed and solid histograms, respectively. This ratio is based on average  $p_T$  spectra (preliminary) of particle and anti-particle measured (open stars) by ALICE Collaboration [75, 76]. In the calculations we take into account the variation of strong color (electric) field with energy. The assumed effective value of the string tension is  $\kappa = 2$  GeV/fm (panel e) corresponding to  $\kappa(s) = \kappa_0 (s/s_0)^{0.04}$  GeV/fm (see Eq. 4). Since we expect in high multiplicity proton-proton collisions features that are similar to those observed in Pb - Pb collisions [1, 3, 8, 18], we consider also the results obtained for an enhanced value of effective string tension to  $\kappa = 5$  GeV/fm (see panel f). The agreement with the data is fairly good in the limit of the error bars, except for very low  $p_T < 1$  GeV values. The experimental spectra show a small depletion at high multiplicity at very low  $p_T$ , indicating possible influence of the radial flow. The transverse momentum spectra of identified particles carrying light quarks and their azimuthal distributions are well described by hydrodynamical models [14, 15] at very low  $p_T$ . However, as far as in the string model the pressure is not considered, it is

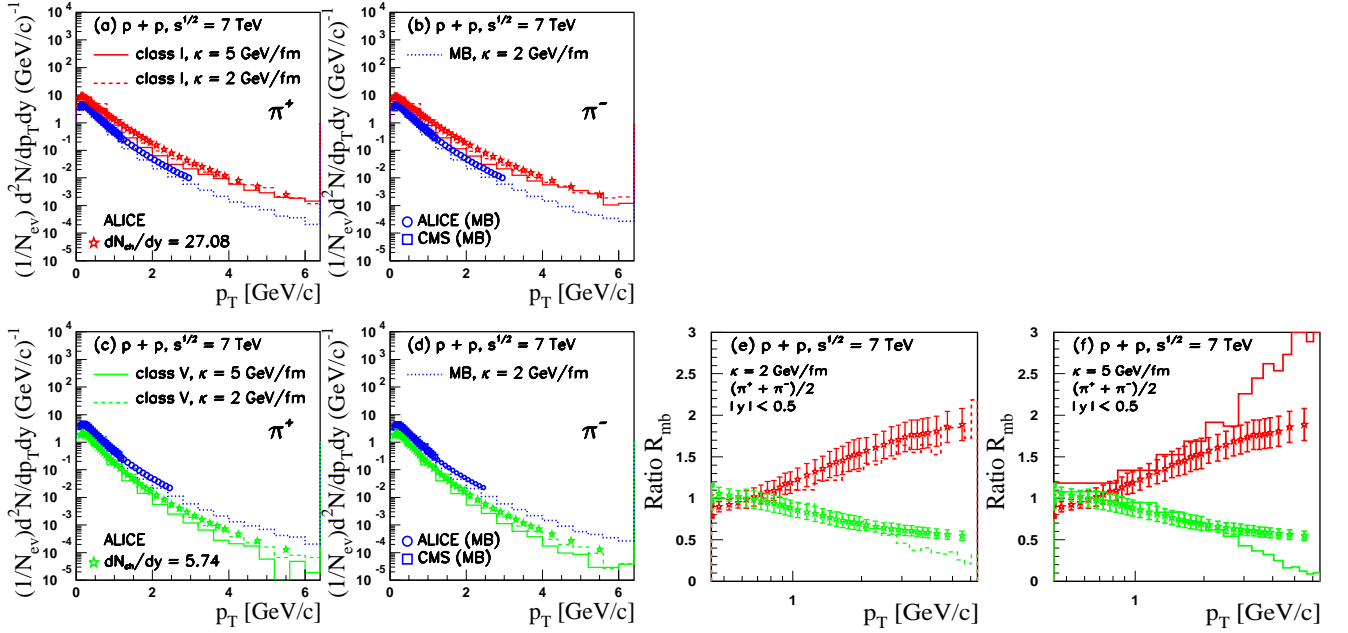


FIG. 5. HIJING/BB v2.0 results for transverse momentum ( $p_T$ ) distributions at mid-rapidity for charged pions in two multiplicity classes (see text for explanation). The results for High (Low) multiplicity class of events are presented in the panels a,b and panels c,d, respectively. The solid (dashed) histograms are obtained using  $\kappa = 5$  GeV/fm ( $\kappa = 2$  GeV/fm) for High (class I) and Low (class V) multiplicity class of events. The results for minimum bias  $pp$  collisions obtained for  $\kappa = 2$  GeV/fm (dotted histograms) are included and compared to data from ALICE [92] (open circles) and CMS Collaborations [97] (open squares). Panel e (f) include the ratios  $R_{mb}$  obtained using  $\kappa = 2$  GeV/fm ( $\kappa = 5$  GeV/fm) respectively. The upper dashed and solid histograms are for HM (class I), and the lower dashed and solid histograms are for LM (class V) class of events. The experimental ratio  $R_{mb}$  was calculated by us based on average  $p_T$  spectra of particle and anti-particle measured (open stars) by ALICE Collaboration [75, 76]. Only statistical error bars are shown.

not expected to describe such effects which could originate from collective expansion. At low and intermediate  $p_T$  ( $1 \text{ GeV/c} < p_T < 6 \text{ GeV/c}$ ), the non-perturbative production mechanism via SCF produces a clear split between High and Low multiplicity events. For the highest multiplicity (class I), we see a hardening of the  $p_T$  spectra for  $\pi, K, p$  and their anti-particles. However, the model predictions could not disentangle between the two considered scenarios. The calculated  $R_{mb}$  ratio is similar for both results obtained with  $\kappa = 2$  GeV/fm and  $\kappa = 5$  GeV/fm, and within experimental errors we can not rule out any of them. These calculations does not show any sensitivity to possible dependence on multiplicity of the effective string tension value,  $\kappa$ .

The HIJING/BB v2.0 model has successfully described the global observables and identified particle (ID) data, including (multi)strange particles production in  $p+p$  [65, 69]  $p - \text{Pb}$  [68, 70] and  $\text{Pb} - \text{Pb}$  collisions [67] at the LHC energies. We will explore here dynamical effects associated with long range coherent fields (*i.e.* strong color fields, SCF, with emphasis on the novel observables (ratio  $R_{mb}$ ) and their multiplicity dependence for (multi)strange particles in  $p+p$  collisions at  $\sqrt{s} = 7$  TeV. Due to strange quark content of (multi)strange particle the study of the ratio  $R_{mb}$  is of particular inter-

est. Since we expect higher sensitivity to SCF effects for (multi)strange than for bulk particles, measurements of  $p_T$  distributions at mid-rapidity as well as the ratio  $R_{mb}$  could help to evidenciate these effects, within the phenomenology embedded in HIJING/BB v2.0 model.

Figure 8 show the ratios of the normalized  $p_T$  distributions,  $R_{mb}$  of  $\Lambda + \bar{\Lambda}$  produced in  $p+p$  collisions at  $\sqrt{s} = 7$  TeV. The results for six multiplicity classes (class I to class VI) based on average  $p_T$  spectra of particle and anti-particle are included. From top to bottom the calculations correspond to highest (class I) to lowest (class VI) multiplicity events. Left (Right) panels are the results obtained with  $\kappa = 2$  GeV/fm ( $\kappa = 5$  GeV/fm) respectively. We remark a clear hardening of the  $p_T$  spectra for high multiplicity, especially for  $N_{ch} > 100$  (class III to class I events), where a change in the slope is obvious. The effect is more evident for an enhanced effective value of string tension  $\kappa = 5$  GeV/fm (see Fig. 8 right panel). Similar results (not included here) are obtained for multi-strange particles, *i.e.*,  $\Xi$  and  $\Omega$ . High multiplicity events have a higher fraction of heavier particles, meaning with a higher strangeness content. We can explain this fact as an effect of strong color field embedded in our model. Note, that  $N_{ch} > 120$  is also the charged particle multiplicity above which was observed the enhancement in the

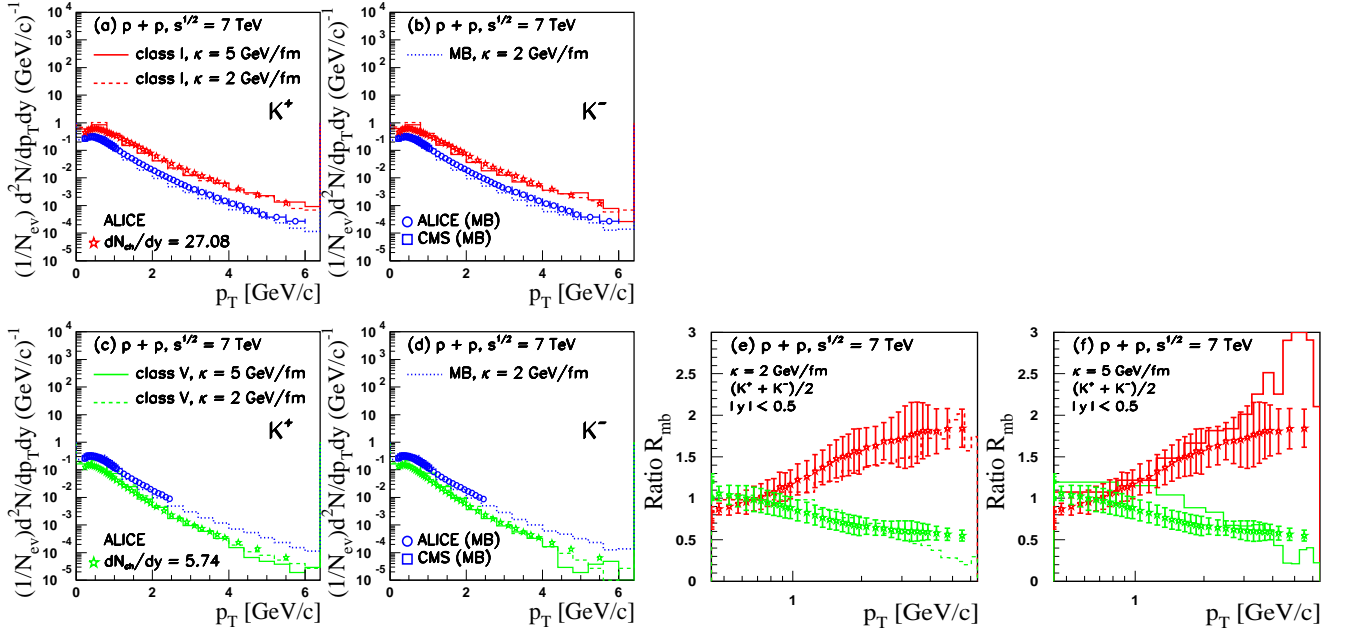


FIG. 6. The same as in Fig. 5 for charged kaons.

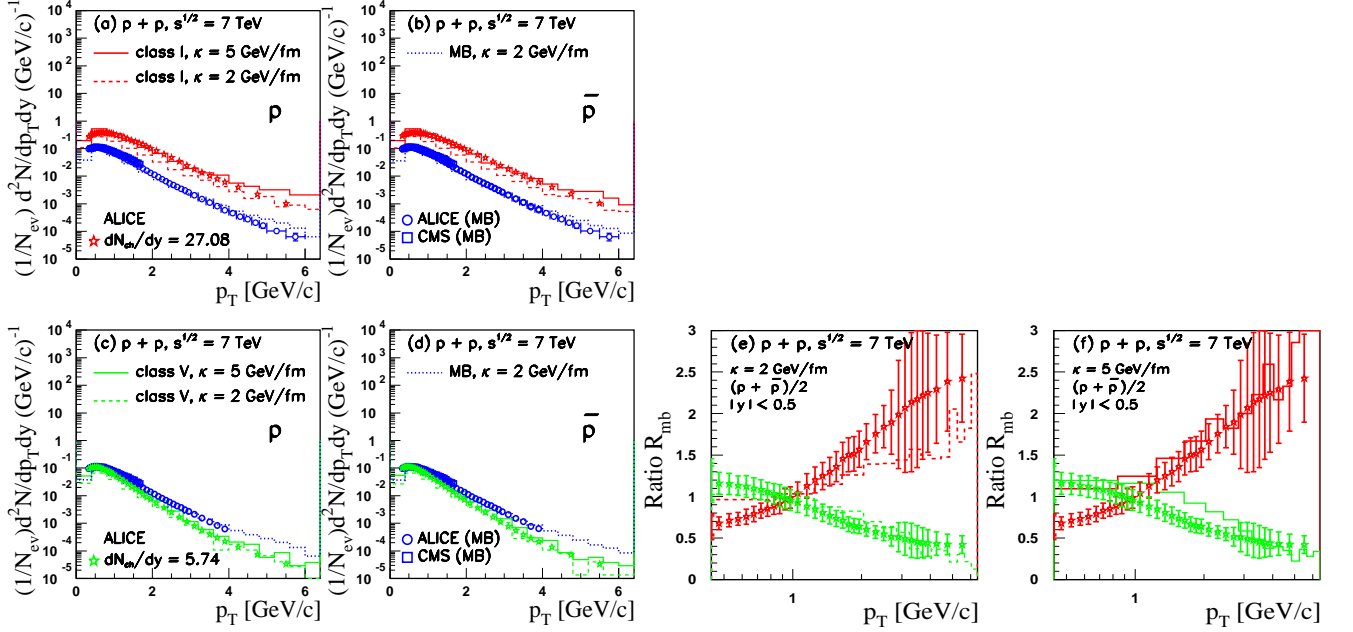


FIG. 7. The same as in Fig. 5 for protons and anti-protons.

near side long range two-particle correlation reported by CMS Collaboration [3]. However, there is no mechanism that produces a ridge in our model.

The experimental fact that  $pp$  collisions manifest features similar with Pb - Pb collisions [3–10, 99] point out to the necessity to modify  $\kappa$ , in describing observables in  $pp$  collisions for HM class of events. The calculations with SCF contributions assume an effective string tension

value  $\kappa = 2$  GeV/fm, obtained from an energy depend  $\kappa$  (see Sec. II), while the results with  $\kappa = 5$  GeV/fm are obtained based on the above experimental fact. Note, that a specific size dependent  $\kappa = \kappa(r)$  was considered recently in PYTHIA 8 model, with  $r$  a new parameter fixed to fit data [12].

Therefore, in Fig. 9 ( $\Lambda$  and  $\bar{\Lambda}$ ), Fig. 10 ( $\Xi^-$  and  $\bar{\Xi}^+$ ), and Fig. 11 ( $\Omega^-$  and  $\bar{\Omega}^+$ ) we show the results obtained for

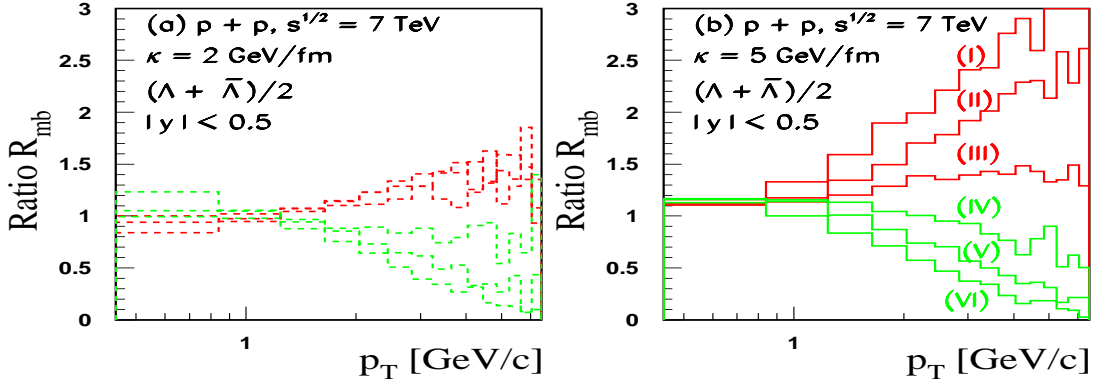


FIG. 8. The HIJING/BB v2.0 model predictions for  $\Lambda + \bar{\Lambda}$  produced in  $pp$  collisions at  $\sqrt{s} = 7$  TeV. The ratios of the normalized  $p_T$  distributions,  $R_{mb}$  (see Eq. 1) for six multiplicity classes (see text for explanation) based on average  $p_T$  spectra of particle and anti-particle. From top to bottom the calculations correspond to class (I) to class (VI) multiplicity events. Left-the results obtained with  $\kappa = 2$  GeV/fm; Right- the results obtained with ( $\kappa = 5$  GeV/fm).

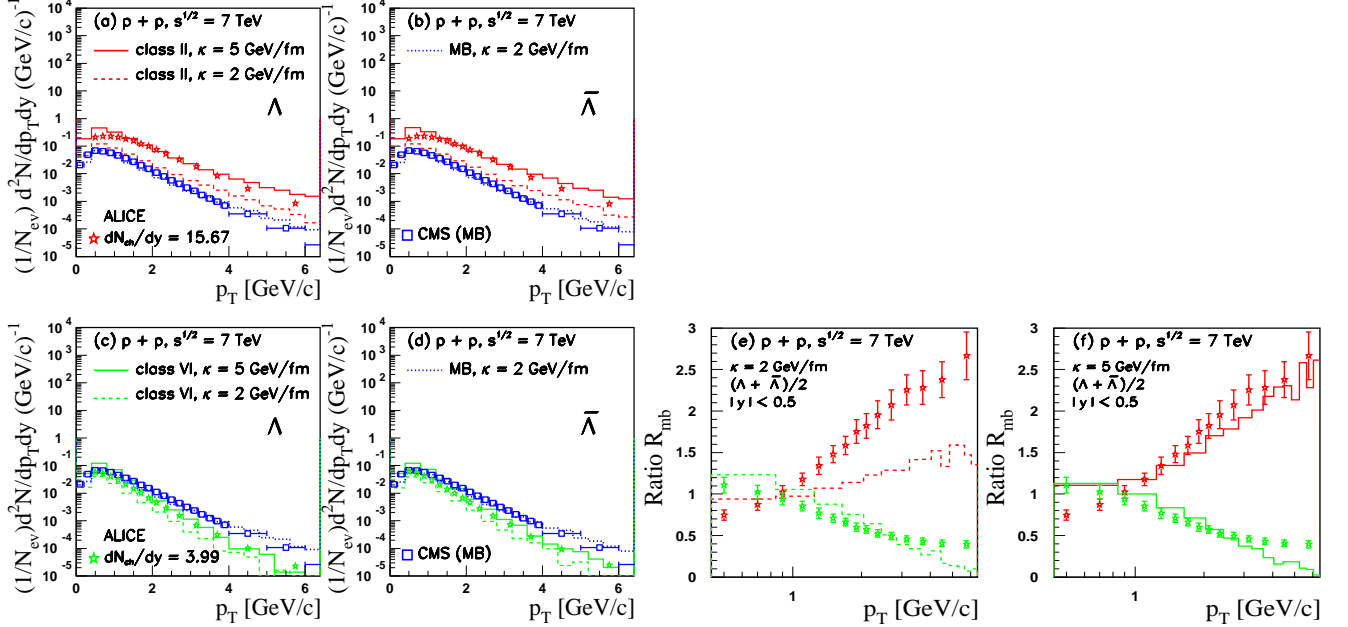


FIG. 9. The same as in Fig. 5 for events of high (class II) and low (class VI) multiplicity. The calculations are for  $\Lambda$  and  $\bar{\Lambda}$ . The results for minimum bias  $pp$  collisions obtained with  $\kappa = 2$  GeV/fm (dotted histograms) are included and compared to data from CMS Collaborations [97] (open squares). Only statistical error bars are shown.

$p_T$  distributions at mid-rapidity for (multi)strange particles in two event classes, corresponding to high (HM) and low (LM) multiplicity. The calculations for minimum bias events are included and compared to data from Refs. [74, 75, 97]. As in the previous calculations comparison to data for HM and LM events, is made for  $p_T$  spectra obtained for a class of multiplicity events which give a value of  $dN_{ch}^{th}/d\eta$  similar with those obtained in the experiment  $\langle dN_{ch}^{exp}/d\eta \rangle$ . Theoretical predictions for the  $p_T$  dependence of  $R_{mb}$  for  $\Lambda + \bar{\Lambda}$ ,  $\Xi^- + \bar{\Xi}^+$ , and  $\Omega^- + \bar{\Omega}^+$  are presented for two scenarios: using  $\kappa = 2$  GeV/fm

(panel e) and an increased value to  $\kappa = 5$  GeV/fm (panel f). The results show a clear hardening of  $p_T$  spectra in case of HM class of events. Moreover, in case of the LM class of events, the  $R_{mb}$  ratio of (multi)strange particles are better described using  $\kappa = 2$  GeV/fm. In contrast, an increase of effective value  $\kappa$  to  $\kappa = 5$  GeV/fm better describes class with HM events. The remark is true for strange  $\Lambda + \bar{\Lambda}$  as well as for multi-strange ( $\Xi^- + \bar{\Xi}^+$ ,  $\Omega^- + \bar{\Omega}^+$ ) particle in  $pp$  collisions at  $\sqrt{s} = 7$  TeV.

To conclude, for a better description of (multi)strange particle productions we have to consider an increase of

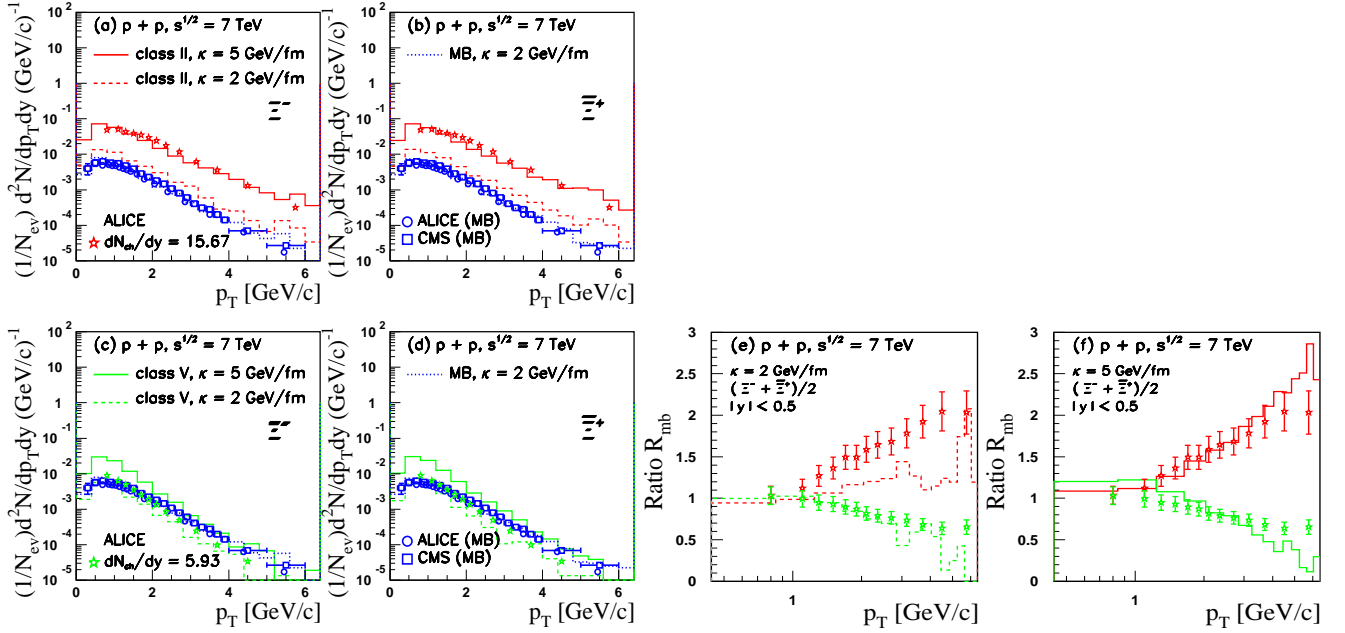


FIG. 10. The same as Fig.5 for events of high (class II) and low (class V) multiplicity. The calculations are for  $\Xi^-$  and  $\Xi^+$ . The results for minimum bias  $pp$  collisions obtained with  $\kappa = 2$  GeV/fm (dotted histograms) are included and compared to data from ALICE [74, 75] (open circles) and CMS Collaborations [97] (open squares). Only statistical error bars are shown.

effective string tension value from  $\kappa = 2$  GeV/fm to  $\kappa = 5$  GeV/fm, which is strongly supported by data. The fact that an effective value  $\kappa = 5$  GeV/fm describes better the  $R_{mb}$  ratio in  $pp$  collisions at  $\sqrt{s} = 7$  TeV, reveal features similar with those observed in chromoelectric flux configurations used to describe some experimental observables in Pb - Pb collisions at  $\sqrt{s_{NN}} = 2.76$  TeV [66]. The enhancement of (multi)strange hadron yields as function of multiplicity have been associated with the creation of a strongly interacting medium, sQGP [91]. Recently, a similar behavior was also observed for multi-strange hadrons in high-multiplicity  $pp$  collisions [10] and this observation challenge all string fragmentation models [12]. Finally, we remark that for  $pp$  collisions at  $\sqrt{s} = 7$  TeV our model predicts higher sensitivity to SCF effects for ID (multi)strange ( $\Lambda$ ,  $\Xi$ ,  $\Omega$ ) than for light hadrons ( $\pi$ ,  $K$ ,  $p$ ). The calculations assuming an effective string tension value which vary only with energy as  $\kappa(s) = \kappa_0 (s/s_0)^{0.04}$  GeV/fm describe fairly well the (multi)strangeness production in the LM event classes, but fail to describe (multi)strange production in HM event classes. A better description is obtained for an enhanced effective string tension value  $\kappa = 5$  GeV/fm which point out to the necessity of a new dependency on multiplicity (or  $\epsilon_{ini}$ ) for the effective string tension value,  $\kappa$ .

#### IV. SUMMARY AND CONCLUSIONS

In summary, we studied in the framework of the HIJING/B $\bar{B}$  v2.0 model, the influence of possible strong homogeneous constant color electric fields on new experimental observables measured by ALICE Collaboration, especially for identified particle in  $pp$ ,  $p$  - Pb, and Pb - Pb collisions at  $\sqrt{s} = 7$  TeV,  $\sqrt{s_{NN}} = 5.02$  TeV, and  $\sqrt{s_{NN}} = 2.76$  TeV, respectively. The effective string tension  $\kappa$ , control  $Q\bar{Q}$  pair creation rates and the suppression factors  $\gamma_{Q\bar{Q}}$ . The measured average transverse momentum and ratio  $R_{mb}$  of ID particle help to verify our assumptions and to set the strangeness suppression factor. We assume in our calculations an energy and possible system dependence of the effective string tension,  $\kappa$ .

For Pb - Pb collisions at  $\sqrt{s_{NN}} = 2.76$  TeV all nuclear effects included in the model, *e.g.*, strong color fields, shadowing and quenching should be taken into account. However, partonic energy loss and jet quenching process as embedded in the model achieve a reasonable description of the  $p_T$  distributions of light hadrons ( $\pi$ ,  $K$ ,  $p$ ). The discrepancy could be explained by an initial condition with a large pressure and therefore a large collective flow, which is not embedded in our model.

For identified particle in  $pp$  collisions at  $\sqrt{s} = 7$  TeV we compute correlation between mean transverse momentum and multiplicity of charged particles ( $N_{ch}^*$ ) at central rapidity as well as the ratio of double differential cross sections normalized to the charged particle densities versus multiplicity,  $R_{mb}$ . In the calculations we

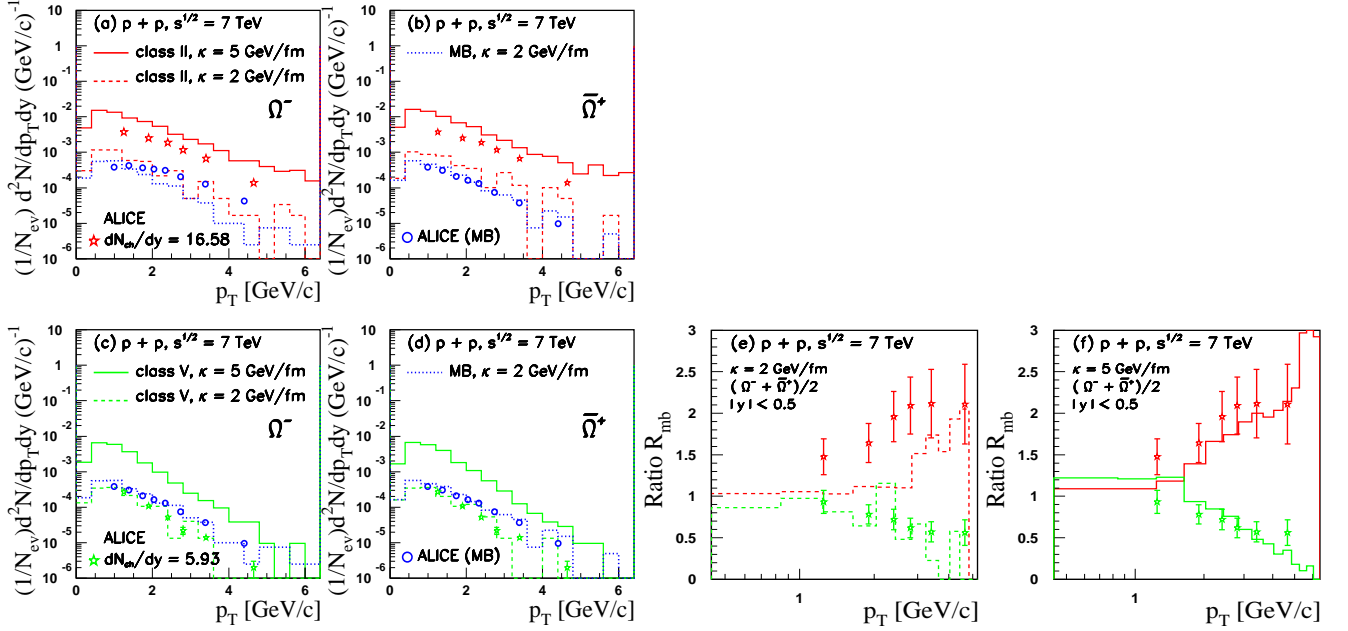


FIG. 11. The same as in Fig. 5 for events of high( class II) and low (class V) multiplicity. The calculations are for  $\Omega^-$  and  $\bar{\Omega}^+$ . The results for minimum bias  $pp$  collisions obtained with  $\kappa = 2$  GeV/fm (dotted histograms) are included and compared to data (open circles) from ALICE [74, 75]. Only statistical error bars are shown.

take into account the variation of strong color (electric) field with energy but not with the multiplicity (or initial energy densities,  $\epsilon_{\text{ini}}$ ) of the colliding system. The assumed effective string tension is  $\kappa = 2$  GeV/fm, corresponding to  $\kappa(s) = \kappa_0 (s/s_0)^{0.04}$  GeV/fm (see Eq. 4). Since we expect in high multiplicity proton-proton collisions features that are similar to those observed in Pb - Pb collisions [1, 3, 8, 18], we consider also the results obtained with an enhanced value of the effective string tension, from  $\kappa = 2$  GeV/fm to  $\kappa = 5$  GeV/fm. This increase of the strength of color fields lead to a ratio  $R_{mb}$  consistent with recent data for HM class of events, while in the LM class of events  $R_{mb}$  is better described using a lower effective string tension value  $\kappa = 2$  GeV/fm. These results show that the above increase of the strength of color fields could be an important dynamical mechanisms. New measurements with high statistics at low and intermediate  $p_T$  ( $1 < p_T < 6$  GeV/c) of the ratio  $R_{mb}$  in  $pp$  collisions at LHC energies, could help to disentangle between different model approaches and/or different

dynamical mechanisms, especially for high multiplicity event classes.

Note, that the HIJING/B $\bar{B}$  model is based on a time-independent strength of color field, while in reality the production of  $Q\bar{Q}$  pairs is more complex being far-from-equilibrium, time and space dependent phenomenon. To achieve more quantitative conclusions, such time and space dependent mechanisms [34, 78] should be considered in future generations of Monte Carlo codes.

## V. ACKNOWLEDGMENTS

One of us (VTP) would like to acknowledge useful discussions with Miklos Gyulassy and Jean Barrette in the early phase of analysis. This work was supported by the Natural Sciences and Engineering Research Council of Canada, and by the Projects number 44/05.10.2011 and 4/16.03.2016 of the Ministry of Research and Innovation via CNCSI and IFA coordinating agencies.

- 
- [1] J. Schukraft, Nucl. Phys. A **967**, 1 (2017).
  - [2] P. Koch, B. Müller and J. Rafelski, Int. J. Mod. Phys. A **32**, 1730024 (2017).
  - [3] V. Khachatryan *et al.*, CMS Collaboration, JHEP **1009**, 091 (2010).
  - [4] S. Chatrchyan *et al.*, CMS Collaboration, Phys. Lett. B **718**, 795 (2013).

- [5] B. Abelev *et al.*, ALICE Collaboration, Phys. Lett. B **719**, 29 (2013).
- [6] G. Aad *et al.*, ATLAS Collaboration, Phys. Lett. B **725**, 60 (2013).
- [7] C. Andrei, ALICE Collaboration, Nucl. Phys. A **931**, 888 (2014).

- [8] G. Aad *et al.*, ATLAS Collaboration, Phys. Rev. Lett. **116**, no. 17, 172301 (2016).
- [9] M. Witek, LHCb Collaboration, EPJ Web Conf. **141**, 01007 (2017).
- [10] J. Adam *et al.*, ALICE Collaboration, Nature Phys. **13**, 535 (2017).
- [11] S. Schlichting and P. Tribedy, Adv. High Energy Phys. **2016**, 8460349 (2016).
- [12] N. Fischer and T. Sjöstrand, JHEP **1701**, 140 (2017).
- [13] C. Bierlich, G. Gustafson and L. Lnnblad, Phys. Lett. B **779**, 58 (2018).
- [14] T. Pierog, I. Karpenko, J. M. Katzy, E. Yatsenko and K. Werner, Phys. Rev. C **92**, no. 3, 034906 (2015).
- [15] K. Werner, B. Guiot, I. Karpenko and T. Pierog, Phys. Rev. C **89**, no. 6, 064903 (2014).
- [16] K. Werner, B. Guiot, I. Karpenko and T. Pierog, Nucl. Phys. A **931**, 83 (2014).
- [17] M. Petrovici, I. Berceanu, A. Pop, M. Târziă and C. Andrei, Phys. Rev. C **96**, no. 1, 014908 (2017).
- [18] C. Loizides, Nucl. Phys. A **956**, 200 (2016).
- [19] B. Nachman and M. L. Mangano, Eur. Phys. J. C **78**, no. 4, 343 (2018).
- [20] W. Li, Nucl. Phys. A **967**, 59 (2017).
- [21] M. Vasilieiou, ALICE Collaboration, EPJ Web Conf. **126**, 04052 (2016).
- [22] S. M. Troshin and N. E. Tyurin, arXiv:1711.01069 [hep-ph].
- [23] R. Acconcia, D. D. Chinellato, R. Derradi de Souza, J. Takahashi, G. Torrieri and C. Markert, Phys. Rev. D **97**, no. 3, 036010 (2018).
- [24] J. S. Schwinger, Phys. Rev. **82**, 664 (1951).
- [25] T. S. Biro, H. B. Nielsen, and J. Knoll, Nucl. Phys. **B245**, 449 (1984).
- [26] M. Gyulassy and A. Iwazaki, Phys. Lett. B **165**, 157 (1985).
- [27] N. Tanji, Annals Phys. **324**, 1691 (2009).
- [28] R. Ruffini, G. Vereshchagin and S. -S. Xue, Phys. Rept. **487**, 1 (2010).
- [29] L. Labun and J. Rafelski, Phys. Rev. D **79**, 057901 (2009).
- [30] N. Cardoso, M. Cardoso and P. Bicudo, Phys. Lett. B **710**, 343 (2012).
- [31] G. C. Nayak, Phys. Rev. D **72**, 125010 (2005).
- [32] G. C. Nayak and P. van Nieuwenhuizen, Phys. Rev. D **71**, 125001 (2005).
- [33] P. Levai and V. Skokov, J. Phys. G **36**, 064068 (2009).
- [34] P. Levai and V. Skokov, Phys. Rev. D **82**, 074014 (2010).
- [35] P. Levai and V. V. Skokov, AIP Conf. Proc. **1348**, 118 (2011).
- [36] P. Levai, D. Berenyi, A. Pasztor and V. V. Skokov, J. Phys. G **38**, 124155 (2011).
- [37] B. Andersson, G. Gustafson, G. Ingelman and T. Sjöstrand, Phys. Rept. **97**, 31 (1983).
- [38] X. -N. Wang and M. Gyulassy, Phys. Rev. Lett. **68**, 1480 (1992); *ibid.* Phys. Rev. D **44**, 3501 (1991).
- [39] X. N. Wang and M. Gyulassy, Phys. Lett. B **282**, 466 (1992).
- [40] F. Gelis, T. Lappi and L. McLerran, Nucl. Phys. **A828**, 149 (2009); T. Lappi and L. McLerran, Nucl. Phys. **A772**, 200 (2006).
- [41] L. McLerran, J. Phys. G **35**, 104001 (2008).
- [42] D. Kharzeev, E. Levin and K. Tuchin, Phys. Rev. C **75**, 044903 (2007).
- [43] M. A. Braun, C. Pajares and V. V. Vechernin, Nucl. Phys. A **906**, 14 (2013).
- [44] H. Sorge, M. Berenguer, H. Stoecker and W. Greiner, Phys. Lett. B **289**, 6 (1992).
- [45] S. A. Bass *et al.*, Prog. Part. Nucl. Phys. **41**, 255 (1998). [Prog. Part. Nucl. Phys. **41**, 225 (1998)].
- [46] M. Bleicher *et al.*, J. Phys. G **25**, 1859 (1999).
- [47] S. Soff *et al.*, J. Phys. G **27**, 449 (2001).
- [48] S. Soff, J. Randrup, H. Stoecker and N. Xu, Phys. Lett. B **551**, 115 (2003).
- [49] Z. W. Lin, C. M. Ko, B. A. Li, B. Zhang and S. Pal, Phys. Rev. C **72**, 064901 (2005).
- [50] M. A. Braun, J. Dias de Deus, A. S. Hirsch, C. Pajares, R. P. Scharenberg and B. K. Srivastava, Phys. Rept. **599**, 1 (2015).
- [51] I. Bautista, PoS ICPAQGP **2015**, 079 (2017).
- [52] C. Merino, C. Pajares, M. M. Ryzhinskiy, Y. .M. Shabelski, and A. G. Shuvaev, Phys. Atom. Nucl. **73**, 1781 (2010), [Erratum-*ibid.* **74**, 173 (2011)].
- [53] I. Bautista and C. Pajares, Phys. Rev. C **82**, 034912 (2010).
- [54] C. Bierlich, G. Gustafson, L. Lnnblad and A. Tarasov, JHEP **1503**, 148 (2015).
- [55] C. Bierlich and J. R. Christiansen, Phys. Rev. D **92**, no. 9, 094010 (2015).
- [56] G. Feofilov, V. Kovalenko and A. Puchkov, arXiv:1710.08895 [hep-ph].
- [57] E. O. Bodnya, V. N. Kovalenko, A. M. Puchkov and G. A. Feofilov, AIP Conf. Proc. **1606**, 273 (2014).
- [58] N. Armesto, D. A. Derkach, and G. A. Feofilov Physics of Atomic Nuclei, **71**, 2087 (2008).
- [59] W. -T. Deng, X. -N. Wang, and R. Xu, Phys. Rev. C **83**, 014915 (2011).
- [60] W. -T. Deng, X. -N. Wang, and R. Xu, Phys. Lett. **B701**, 133 (2011).
- [61] V. Topor Pop, M. Gyulassy, J. Barrette, C. Gale, X. N. Wang, and N. Xu, Phys. Rev. C **70**, 064906 (2004).
- [62] V. Topor Pop, M. Gyulassy, J. Barrette, C. Gale, R. Bellwied, and N. Xu, Phys. Rev. C **72**, 054901 (2005).
- [63] V. Topor Pop, M. Gyulassy, J. Barrette, C. Gale, S. Jeon, and R. Bellwied, Phys. Rev. C **75**, 014904 (2007).
- [64] V. Topor Pop, J. Barrette, and M. Gyulassy, Phys. Rev. Lett. **102**, 232302 (2009).
- [65] V. Topor Pop, M. Gyulassy, J. Barrette, C. Gale, and A. Warburton, Phys. Rev. C **83**, 024902 (2011).
- [66] V. Topor Pop, M. Gyulassy, J. Barrette, C. Gale and M. Petrovici, J. Phys. G **41**, 115101 (2014).
- [67] V. Topor Pop, M. Gyulassy, J. Barrette, and C. Gale, Phys. Rev. C **84**, 044909 (2011).
- [68] G. G. Barnafoldi, J. Barrette, M. Gyulassy, P. Levai, and V. Topor Pop, Phys. Rev. C **85**, 024903 (2012).
- [69] V. Topor Pop, M. Gyulassy, J. Barrette, C. Gale, and A. Warburton, Phys. Rev. C **86**, 044902 (2012).
- [70] J. L. Albacete, N. Armesto, R. Baier, G. G. Barnafoldi, J. Barrette, S. De, W. -T. Deng, and A. Dumitru *et al.*, Int. J. Mod. Phys. E Vol. **22**, 1330007 (2013).
- [71] J. L. Albacete *et al.*, Int. J. Mod. Phys. E **25**, no. 9, 1630005 (2016).
- [72] G. Ripka (ed.), Lecture Notes in Physics (Springer, Berlin, 2004), Vol. **639**, 138 (2004).
- [73] V. K. Magas, L. P. Csernai and D. Strottman, Nucl. Phys. A **712**, 167 (2002).
- [74] L. Bianchi [ALICE Collaboration], Nucl. Phys. A **956**, 777 (2016).

- [75] R. Derradi de Souza [ALICE Collaboration], J. Phys. Conf. Ser. **779**, no. 1, 012071 (2017).
- [76] V. Vislavicius [ALICE Collaboration], Nucl. Phys. A **967**, 337 (2017).
- [77] T. D. Cohen and D. A. McGady, Phys. Rev. D **78**, 036008 (2008).
- [78] F. Hebenstreit, R. Alkofer, and H. Gies, Phys. Rev. D **78**, 061701 (2008).
- [79] K. Nakamura *et al.*, Particle Data Group, J. Phys. G **37**, 075021 (2010).
- [80] M. Cristoforetti, P. Faccioli, G. Ripka, and M. Traini, Phys. Rev. D **71**, 114010 (2005).
- [81] N. S. Amelin, N. Armesto, C. Pajares, and D. Sousa, Eur. Phys. J. C **22**, 149 (2001).
- [82] L. McLerran and M. Praszalowicz, Acta Phys. Polon. B **41**, 1917 (2010).
- [83] K. Aamodt *et al.* [ALICE Collaboration], Phys. Rev. Lett. **105**, 252301 (2010).
- [84] B. Abelev *et al.* [ALICE Collaboration], Phys. Rev. Lett. **110**, 032301 (2013).
- [85] B. Andersson, G. Gustafson, and B. Nilsson-Almqvist, Nucl. Phys. **B281**, 289 (1987); B. Nilsson-Almqvist and E. Stenlund, Comput. Phys. Commun. **43**, 387 (1987).
- [86] H. -U. Bengtsson and T. Sjöstrand, Comput. Phys. Commun. **46**, 43 (1987).
- [87] T. Sjöstrand, S. Mrenna, and P. Z. Skands, JHEP **0605**, 026 (2006).
- [88] B. B. Abelev *et al.*, ALICE Collaboration, Phys. Lett. B **727**, 371 (2013).
- [89] J. Liao and E. Shuryak, Phys. Rev. D **82**, 094007 (2010).
- [90] O. Kaczmarek and F. Zantow, Phys. Rev. D **71**, 114510 (2005).
- [91] B. B. Abelev *et al.* [ALICE Collaboration], Phys. Lett. B **728**, 25 (2014).
- [92] J. Adam *et al.* [ALICE Collaboration], Eur. Phys. J. C **75**, no. 5, 226 (2015).
- [93] T. Alexopoulos *et al.*, Phys. Rev. Lett. **64**, 991 (1990).
- [94] J. D. Bjorken, Preprint FERMILAB-PUB-82-059-THY (1982).
- [95] L. Van Hove, Phys. Lett. B **118**, 138 (1982).
- [96] Renato Campanini, Gianluca Ferri, Phys. Lett. B **703**, 237 (2011).
- [97] S. Chatrchyan *et al.* [CMS Collaboration], Eur. Phys. J. C **72**, 2164 (2012).
- [98] B. B. Abelev *et al.*, ALICE Collaboration, Phys. Lett. B **736**, 196 (2014).
- [99] M. Petrovici, A. Lindner, A. Pop, M. Târziă and I. Berceanu, arXiv:1805.04060 [hep-ph].